# MICROFACIES ANALYSIS AND PALEOENVIRONMENTAL TRENDS OF THE PALEOCENE FARRUD AND MABRUK RESERVOIRS, CONCESSION 11, WEST SIRT BASIN, LIBYA

Nisreen Agha*, Amin Gheith**, Salah El-Beialy**, Haitham El-Atfy** and Waleed Shukri**

**Abstract:** Investigation of thin sections taken from representative core samples under the petrological microscope reveals common petrographic and mineralogical characteristics with distinct faunal assemblages allow establishing the microfacies associations and deducing the paleoenvironmental trends of the Paleocene Farrud and Mabruk rock units. Recognition of the early and post diagenetic processes particularly dolomitization and micritization as well as dissolution and precipitation of spary drusy calcite as a newmorphism process affecting the reservoir rocks is established. The microfacies trends detected from the investigation of 46 core samples from Farrud Member (Lower Paleocene) representing six wells; QQQ1-11, GG1-11, LLL1-11, RRR1-11, RRR40-11 and RRR45-11 indicate that the deposition was started within the realm of shallow supratidal and intertidal subenvironments followed by deeper environments of the shelf bays with maximum sea level during inner shelf environment where fossiliferous bioclastic packstone dominated. The microfacies associations determined in 8 core samples from two wells LLL1and RRR40 representing Mabruk Member (Upper Paleocene) indicate paleoenvironmental trends marked by sea level fluctuations accompanied with a relatively marine shelf bay conditions intervened with short-lived shallow intertidal and supratidal warm coastal sedimentation. As a result dolostone, evaporitic dismicrites and gypsiferous dolostone of supratidal characters were deposited.

**Keywords**: Farrud and Mabruk memebers, Paleocene, microfacies associations, diagenesis, sea level oscillation, and depositional environments.

## INTRODUCTION

The Sirt Basin is the youngest sedimentary basin in Libya, one of Africa's most productive petroleum basins, and the world's 13th largest petroleum province. The vast majority of hydrocarbons recovered from Libya have been exploited in the basin, making it of a great economic importance and attracting the attention of many explorationists and petroleum companies. The Sirt Basin is separated structurally, by the Zelten platform into the west Sirt Basin (the focus of this study) and the east Sirt Basin (Hallett, 2002). The area of study is located onshore north-central Libya, west Concession 11, west of the Sirt Basin. The present paper focuses on Concession 11 (Fig. 1A), which is located in the Zallah Trough in the west of the basin (Figs. 1B and C). This concession includes many giant oil fields (Table1). In this paper, we will deal with the microfacies description of 54 core samples retrieved from Paleocene time, Sirt Basin, NW Libya. The microfacies trends detected from the investigation of 46 core samples from Farrud Member (Lower Paleocene) representing six wells; QQQ1-11, GG1-11, LLL1-11, RRR1-11, RRR40-11 and RRR45-11 and 8 core samples representing Mabruk Member (Upper Paleocene) were investigated from two wells LLL1and RRR40 (Table 2).

## LITHOSTRATIGRAPHY

Stratigraphically, Abadi (2002) classified the deposits of the Sirt Basin into pre-rift (Cambro-Ordovician), syn-rift (Upper Cretaceous-Eocene) and post-rift (Oligo-Miocene).The pre-rift and post-rift deposits were dominated by clastics, whereas

*Harouge Oil Operations, Petroleum Engineering Department, Tripoli, Libya.
**Geology Department, Faculty of Science, Mansoura University, Egypt.
Corresponding author: nisreenagha9@gmail.co.com

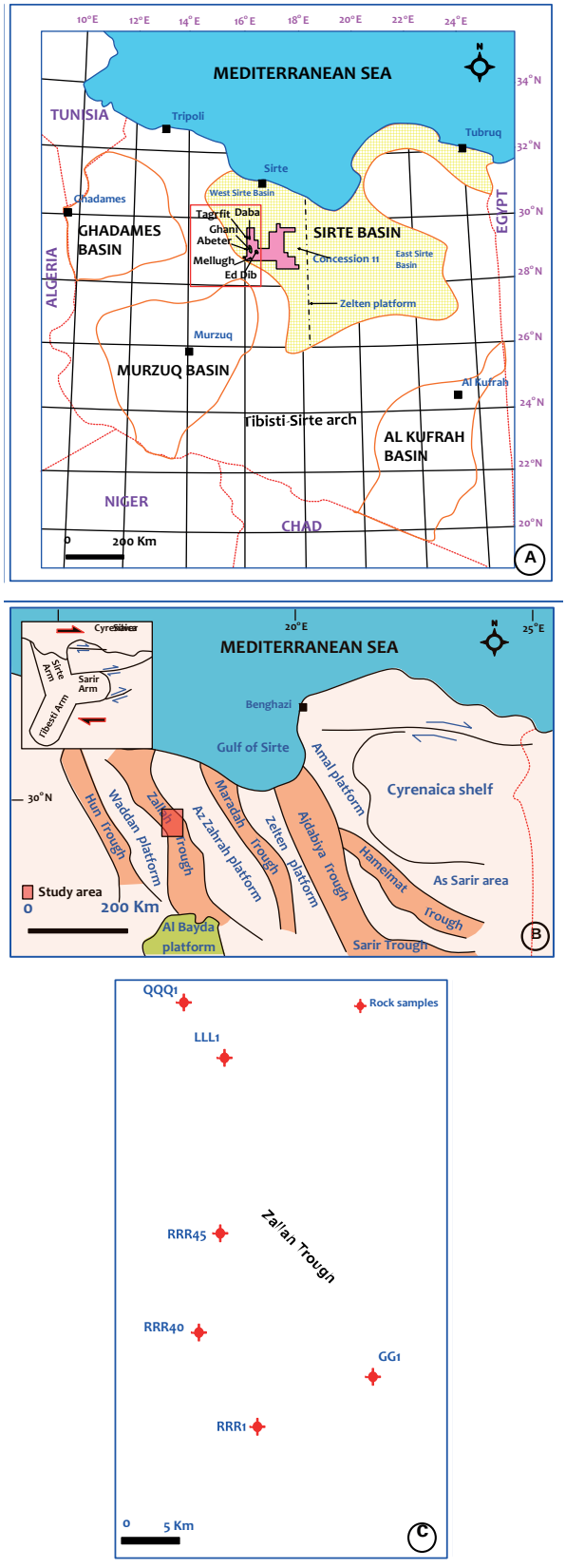


Fig. 1. A. location map of the study area in Concession 11, western Sirt Basin, northern Libya; B: the main structural elements in the Sirt Basin; Fig.1.C, the location of wells studied. Figure after Ahlbrandt (2001), Hallett (2002), and Abadi *et al* (2008).

the syn-rift (Cretaceous- Eocene) sediments were dominated by non-clastics (Fig. 2). The floor of the Sirt Basin is a major unconformity, above which a thick sequence of Late Cretaceous to Recent sediments overlies. The present study is focused on the syn-rift deposits because of the availability of samples and their economic importance as reservoir rocks in the study area. The Paleocene sediments in the Sirt Basin start at the base with the Danian Hagfa Formation. This is followed upward with the Montian Beda Formation and terminated with the Landenian Dahra, Zelten and the lower Kheir formations. The target in this paper is Beda Formation that is consists mainly of various interbedded limestone lithofacies with subordinate dolomite and calcareous shale. The Beda Formation is subdivided into three members from base to top as follow: (1) Thalith Member, (2) Farrud Member, and (3) Mabruk Member. The last two members will be considered in the present study due to their economic importance as reservoir rocks in the study area. The Farrud Member consists of a regressive carbonate depositional cycle at the base, whereas in its upper part fine grained sediments, grade upward to coarser-grained sediments. The latter were deposited in shallower and more agitated water (HOO, 2009). This is followed upward by the deposition of the Mabruk Member (HOO, 2009).

## STRUCTURAL FRAMEWORK

The Sirt Basin is one of the important structural features in north Libya. The Sirt Basin is heavily fractured with major faults resulting in a number of major NW-SE trending grabens (Fig. 1B). These are from NW to SE: the Dur al Abd, Zallah, Abu Tumayam, Maradah, Ajdabiya, and Hameimat. The platforms on the intervening horst blocks are from the west to east: Waddan Platform, Az Zahrah-Al Hufrah, Al Bayda, Zelten, and Al Jahamah platforms (Abadi, 2002).

## TECTONIC FRAMEWORK

The North African region was subjected to diachronous rifting with subsequent post-Mesozoic continental collision, leading to the development of basins with complex histories. A number of different tectonic domains existed, with each basin having a unique tectonic history (Carr, 2003). The Sirt Basin is a major intracratonic rift system on the north central African Plate and comprises a complex

Table 1. List of the studied wells in the giant oilfields, Concession 11, west Sirt Basin, NW Libya.

| Well name | Field | Coordinates | | Pay zone | Age | Total depth (ft) |
|---|---|---|---|---|---|---|
| | | Lat | Lon | | | |
| QQQ1 | Tagrfit | 29° 17′ 25″ | 17° 23′ 52″ | Farrud | Paleocene | 9490 |
| LLL1 | Daba | 29° 15′ 10″ | 17° 26′ 06″ | Farrud | Paleocene | 10361 |
| RRR45 | Ghani | 29° 61′ 34″ | 17° 27′ 14.5″ | Farrud | Paleocene | 6300 |
| RRR40 | Ghani | 28° 59′ 38.06″ | 17° 25′ 37.7″ | Farrud | Paleocene | 8300 |
| RRR1 | Ghani | 28° 57′ 41.0″ | 17° 28′ 0.0″ | Farrud | Paleocene | 6160 |
| GG1 | Ed- Did | 28° 59′ 34″ | 17° 34′ 08″ | Gir (Facha) | Eocene | 10989 |

of horsts and grabens that began to develop during the latest Jurassic-Early Cretaceous. The tectonic evolution of the Sirt Basin involved thermal arching and repeated phases of rifting that culminated in the Late Cretaceous and Paleocene to Early Eocene, which were followed by thermal subsidence from Late Eocene onwards (Abadi, 2002). The sedimentary succession of the Sirt Basin reflects its tectonic and structural evolution, which is closely related to the opening of the Atlantic Ocean and the convergence of the Tethys in Mesozoic and Tertiary times (Gras and Thusu, 1998).

The Sirt Basin area experienced stretching and down faulting during the Cretaceous. Large scale subsidence and block faulting began in the latest Jurassic/Early Cretaceous (Abugares, 2007). The faults in the Sirt Basin are reactivated during the Late Cretaceous and continuously into the Early Paleocene and Late Eocene, where volcanic activity is resumed in post-Eocene times. This is believed to have been concurrent with movement along major basement fault zones situated outside the Cretaceous rift on the western side of the Sirt Basin. The subsidence of the Sirt Basin reached a maximum during Paleocene/ Eocene time (Gumati and Kanes, 1985).

## MATERIAL AND METHODS

This paper focuses on 6 wells located in Concession11, western Sirt Basin (Fig. 1 A; Table1). Fifty-four rock samples were cut for thin sections using a cut-off saw and ground flat before being impregnated with Epoxy Resin (Table 2). The samples were mounted on glass slides ground and polished using Carbide Grit until they were about 0.03mm thick. Subsequently, the sections were covered with glass cover slips. The standard polarizing microscope Olympus BX51 (E330-ADU1.2X) in plane polarized light (PPL) and between Cross Nicols (XPL) was used for thin sections petrographic analysis and photomicrographs were taken digitally. The focus was to recognize diagenetic components and cements in addition to the identification fossil contents.

A brief review of carbonate classifications was first given by Folk (1959, 1962) based upon their orthochemical and allochemical components, as well as, their textural class.

On the other hand, Dunham's (1962) used a limestone textural and compositional classification; which was modified later on (Embry and Klovan, 1971). Subsequently Flügel (1982, 2004) and Wilson (1975) summarized the standard microfacies types (26 SMF) and facies zones (9 FZ) to identify their related depositional environments. A wide usage of the microfacies analysis took place due to the great progress in oil and gas exploration.

## RESULTS AND DISCUSSION

### Microfacies Characteristics of Lower Paleocene Farrud (Selandian) Member

Forty-six thin sections have been examined from 6 wells including the following: QQQ1 (9 samples), LLL1 (8 samples), RRR45 (11 samples), RRR40 (5 samples), RRR1 (8 samples), and GG1 (5 samples). This member is the most important one in the studied wells because it acts as a reservoir rock in the studied concession. The investigated facies from the above member are described as follow:

Table 2. List of the studied Paleocene samples in six wells, Concession 11, west Sirt Basin, NW Libya.

| Sample No. | Well name | Age | Sample type | Depth (ft) | Rock unit |
|---|---|---|---|---|---|
| 1 | RRR40 | Paleocene (Selandian) | Core | 5968 | **Mabruk Member** |
| 2 | RRR40 | Paleocene (Selandian) | Core | 5972 | **Mabruk Member** |
| 3 | RRR40 | Paleocene (Selandian) | Core | 5978 | **Mabruk Member** |
| 4 | RRR40 | Paleocene (Selandian) | Core | 5989 | **Mabruk Member** |
| 5 | LLL1 | Paleocene (Selandian) | Core | 5280 | **Mabruk Member** |
| 6 | LLL1 | Paleocene (Selandian) | Core | 5289 | **Mabruk Member** |
| 7 | LLL1 | Paleocene (Selandian) | Core | 5297 | **Mabruk Member** |
| 8 | LLL1 | Paleocene (Selandian) | Core | 5298 | **Mabruk Member** |
| 9 | RRR40 | Paleocene (Selandian) | Core | 6090 | **Farrud Member** |
| 10 | RRR40 | Paleocene (Selandian) | Core | 6032 | **Farrud Member** |
| 11 | RRR40 | Paleocene (Selandian) | Core | 6035 | **Farrud Member** |
| 12 | RRR40 | Paleocene (Selandian) | Core | 6041 | **Farrud Member** |
| 13 | RRR40 | Paleocene (Selandian) | Core | 6048 | **Farrud Member** |
| 14 | RRR1 | Paleocene (Selandian) | Core | 5951 | **Farrud Member** |
| 15 | RRR1 | Paleocene (Selandian) | Core | 5954 | **Farrud Member** |
| 16 | RRR1 | Paleocene (Selandian) | Core | 5970 | **Farrud Member** |
| 17 | RRR1 | Paleocene (Selandian) | Core | 5981 | **Farrud Member** |
| 18 | RRR1 | Paleocene (Selandian) | Core | 5984 | **Farrud Member** |
| 19 | RRR1 | Paleocene (Selandian) | Core | 5993 | **Farrud Member** |
| 20 | RRR1 | Paleocene (Selandian) | Core | 5994 | **Farrud Member** |
| 21 | RRR1 | Paleocene (Selandian) | Core | 6003 | **Farrud Member** |
| 22 | RRR45 | Paleocene (Selandian) | Core | 5832 | **Farrud Member** |
| 23 | RRR45 | Paleocene (Selandian) | Core | 5837 | **Farrud Member** |
| 24 | RRR45 | Paleocene (Selandian) | Core | 5840 | **Farrud Member** |
| 25 | RRR45 | Paleocene (Selandian) | Core | 5850 | **Farrud Member** |
| 26 | RRR45 | Paleocene (Selandian) | Core | 5857 | **Farrud Member** |
| 27 | RRR45 | Paleocene (Selandian) | Core | 5861 | **Farrud Member** |
| 28 | RRR45 | Paleocene (Selandian) | Core | 5874 | **Farrud Member** |
| 29 | RRR45 | Paleocene (Selandian) | Core | 5898 | **Farrud Member** |
| 30 | RRR45 | Paleocene (Selandian) | Core | 5944 | **Farrud Member** |
| 31 | RRR45 | Paleocene (Selandian) | Core | 5949 | **Farrud Member** |
| 32 | RRR45 | Paleocene (Selandian) | Core | 5959 | **Farrud Member** |
| 33 | GG1 | Paleocene (Selandian) | Core | 5668 | **Farrud Member** |
| 34 | GG1 | Paleocene (Selandian) | Core | 5670 | **Farrud Member** |
| 35 | GG1 | Paleocene (Selandian) | Core | 5713 | **Farrud Member** |
| 36 | GG1 | Paleocene (Selandian) | Core | 5723 | **Farrud Member** |
| 37 | GG1 | Paleocene (Selandian) | Core | 5798 | **Farrud Member** |
| 38 | QQQ1 | Paleocene (Selandian) | Core | 5402 | **Farrud Member** |
| 39 | QQQ1 | Paleocene (Selandian) | Core | 5404 | **Farrud Member** |
| 40 | QQQ1 | Paleocene (Selandian) | Core | 5405 | **Farrud Member** |
| 41 | QQQ1 | Paleocene (Selandian) | Core | 5406 | **Farrud Member** |
| 42 | QQQ1 | Paleocene (Selandian) | Core | 5410 | **Farrud Member** |
| 43 | QQQ1 | Paleocene (Selandian) | Core | 5418 | **Farrud Member** |
| 44 | QQQ1 | Paleocene (Selandian) | Core | 5420 | **Farrud Member** |

Table 2. Cont.

| | | | | | |
|---|---|---|---|---|---|
| 45 | QQQ1 | Paleocene (Selandian) | Core | 5422 | **Farrud Member** |
| 46 | QQQ1 | Paleocene (Selandian) | Core | 5429 | **Farrud Member** |
| 47 | LLL1 | Paleocene (Selandian) | Core | 5304 | **Farrud Member** |
| 48 | LLL1 | Paleocene (Selandian) | Core | 5314 | **Farrud Member** |
| 49 | LLL1 | Paleocene (Selandian) | Core | 5317 | **Farrud Member** |
| 50 | LLL1 | Paleocene (Selandian) | Core | 5322 | **Farrud Member** |
| 51 | LLL1 | Paleocene (Selandian) | Core | 5326 | **Farrud Member** |
| 52 | LLL1 | Paleocene (Selandian) | Core | 5331 | **Farrud Member** |
| 53 | LLL1 | Paleocene (Selandian) | Core | 5335 | **Farrud Member** |
| 54 | LLL1 | Paleocene (Selandian) | Core | 5337 | **Farrud Member** |

***Dolostone association/Dolomite wackestone (Figs. 3A & B, samples 46, 45, 42, 39, QQQ1 well)***: This microfacies shows medium-sized, equigranular, euhedral to subhedral dolomite crystals as a common groundmass. Many dolomite crystals are stained with dark brown ferruginous matter. The abundance of uni-sized homogeneous rhomboid dolomite crystals suggests that deposition took place within arid tidal flats (Selley, 1980; Reading, 1996). This microfacies resembles SMF23 and FZ9 (Wilson, 1975; Flügel, 2004).

***Anhydrite dolostone association/Anhydrite dolomite wackestone (Figs. 3C & D, samples 44, 43, 41, QQQ1 well)***: It shows medium-sized, mosaic ehudral dolomite crystals as a groundmass. No allochemes present. Most pore spaces and fissures are filled with anhydrite crystal laths with radiating habit, as it is distinguished from gypsum by its higher relief and stronger birefringence. This association suggests deposition within arid, evaporitic supratidal setting. The presence of anhydrite facies indicates super saturated saline-rich sources together with high temperature conditions (Adams *et al*, 1984). It resembles SMF23 and FZ9 (Wilson, 1975; Flügel, 2004).

***Evaporite pelloidal dolostone association/ Evaporite dolomitized wackstone (Fig. 3E, sample 40, QQQ1well)***: Fine to medium-grained rhombic recrystallized dolomite crystals, and abundant pelloidal allochemes composed of micrite lacking any recognizable internal structure. The micritic pellets sometimes show recrystallization of mosaic rhombic dolomite in the internal structure. Some laths of anhydrite and gypsum filling a cavity, occupy fissures and voids as a new diagenetic alteration. The abundance of uni-sized homogeneous rhomboid dolomite crystals indicates deposition within evaporitic, tidal flats and/or supratidal setting. The high salinity within the lagoon allowed no fauna to flourish. This association is similar to SMF23 and FZ8 (Wilson, 1975; Flügel, 2004).

***Evaporite (anhydrite) association (Fig. 3F sample 38, QQQ1 well)***: Recrystallized coarse granular mosaic and large fibrous crystals of anhydrite arranged in parallel orientation. The evaporite facies suggests close nearness to super-saturated saline-rich sources of high intertidal-supratidal flats, together with high temperature conditions (Kinsman, 1969).

***Micritized biodolomite association/Biodolomite wackstone (Fig. 3G, sample 37, GG1 well)***: Compact mosaic anhedral crystals of dolomite embedded in a micritic matrix. The crystal fabric is tightly interlocked with some rhombic-shaped dolomite. Poorly-preserved bivalves and foraminifera are recorded and replaced by mosaic calcite. Ferrugineous materials are seen as clouds staining many parts of dolomite and surrounding the micritized fossils. Deposition within shallow restricted supratidal marine setting is suggested for the present association. This facies is in accordance with SMF23 and FZ9 (Wilson, 1975; Flügel, 2004).

***Ostracodal biomicrite association/Ostracodal wackestone (Fig. 3H, sample 36, GG1 well)***: Turbid micrite with argillaceous and abundant ferruginous materials. The allochems are generally few, represented by different skeletal debris, complete ostracodal shells, few bivalvs and ill-defined foraminiferal chambers are floating in the micritic matrix. Most of the internal cavities of the shells are entirely recrystallized into coarse crystalline mosaic calcite. Deposition prevailed in a relatively shallow marine condition, sluggish

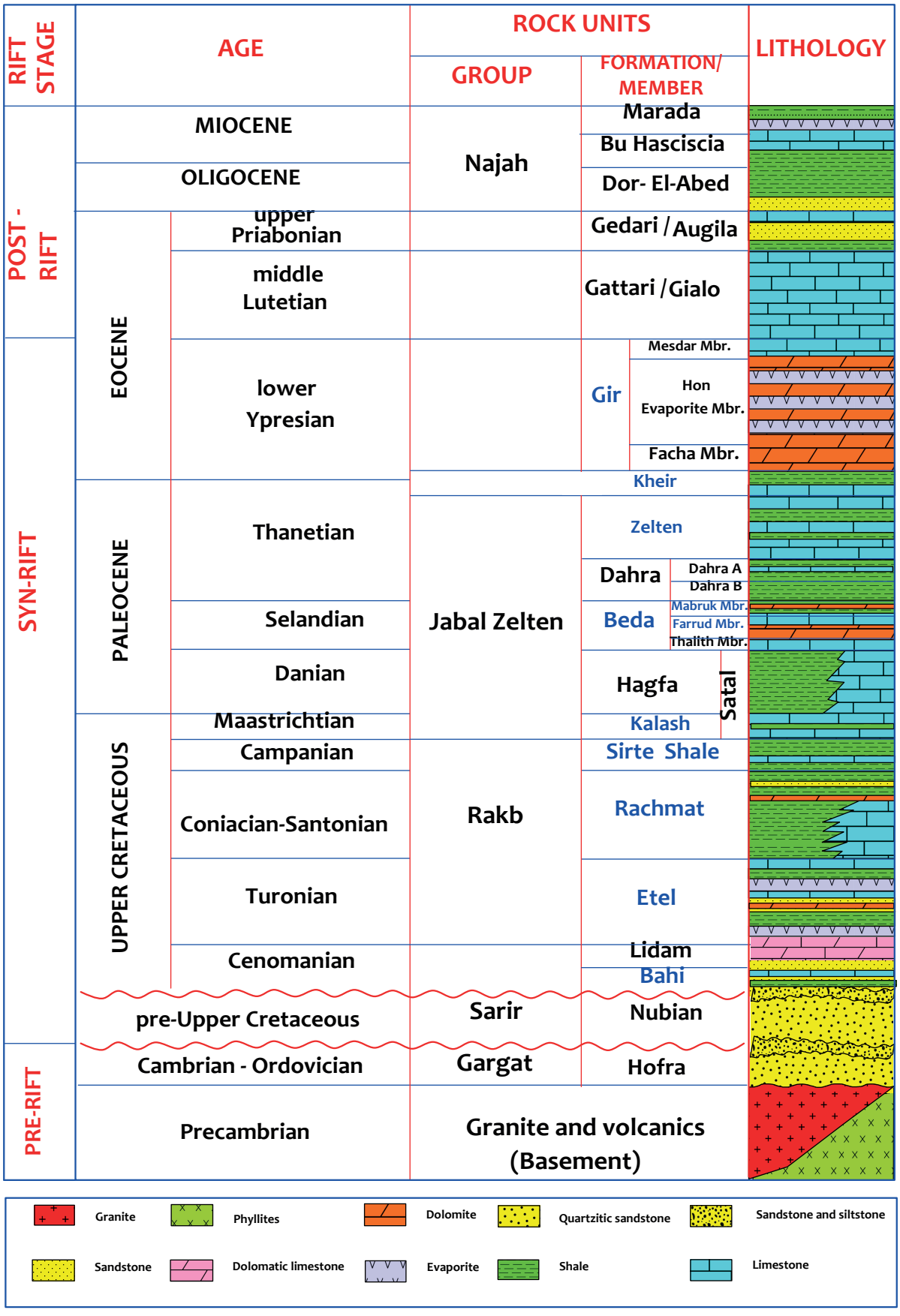


Fig. 2. Generalized lithostratigraphic column for the Concession 11 area, west Sirt Basin, Libya (modified after Barr and Weegar, 1972; Hallett, 2002).

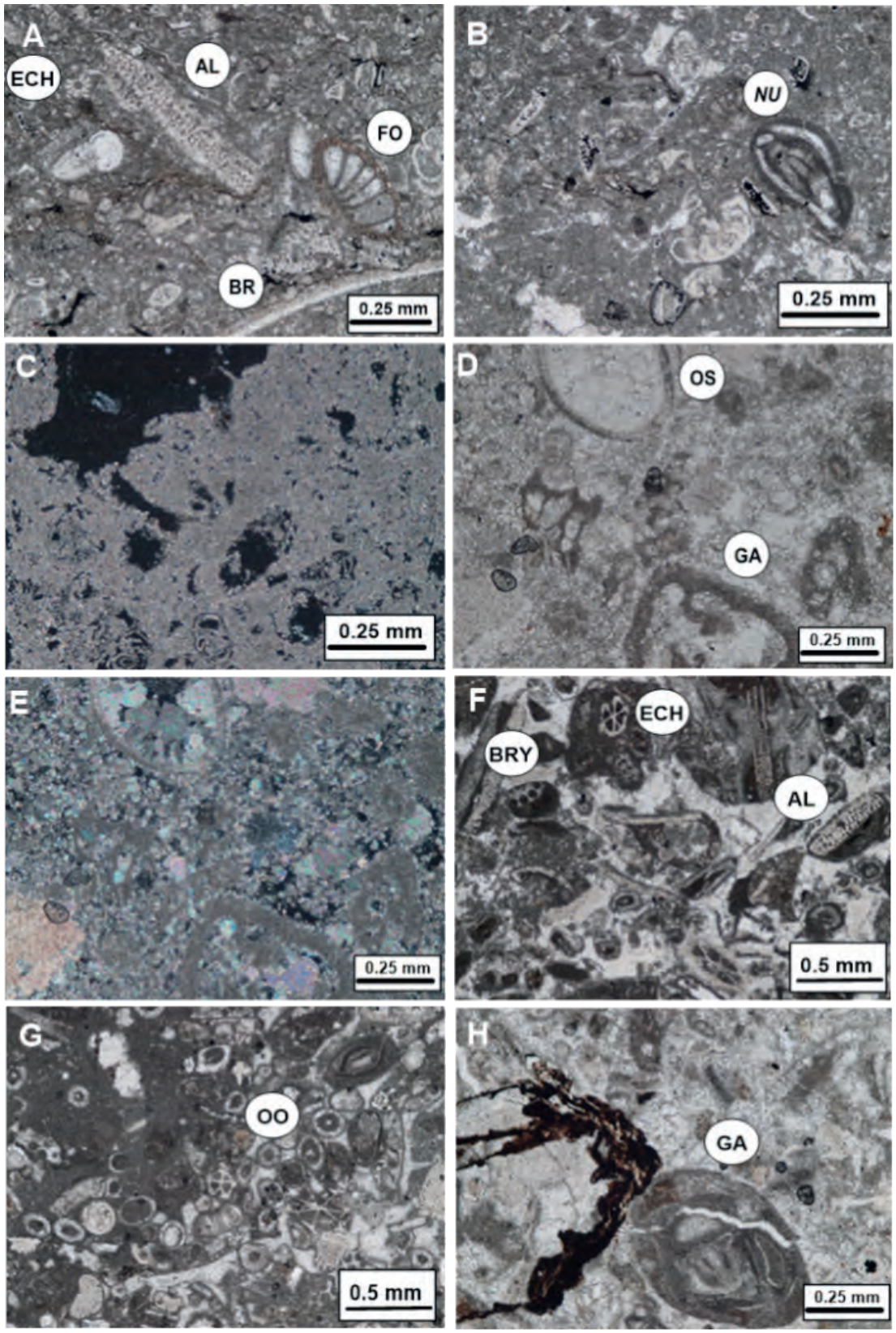


Fig. 3. The Paleocene (Selandian) Farrud Member microfacies; A-B, Dolomite wackestone association, Farrud Member, Paleocene (Selandian), samples 46, 5429 ft, 45, 5422 ft, 42, 5410 ft and 39, 5404 ft, QQQ1 well, XPL. C-D, Anhydrite dolomite wackstone, Farrud Member, samples 44 (5420 ft), 43 (5418 ft) and 41 (5406 ft), QQQ1 well, XPL. E, Evaporite dolomitized wackstone association, sample 40 (5404 ft), QQQ1 well, XPL. F, Evaporite association, sample 38 (5402 ft), QQQ1 well, XPL. G, Micritized biodolomite association, sample 37 (5798 ft), GG1 well, XPL. H, Ostracodal wackestone association. Ostracod shells (OS), sample 36 (5723 ft), GG1 well, XPL.

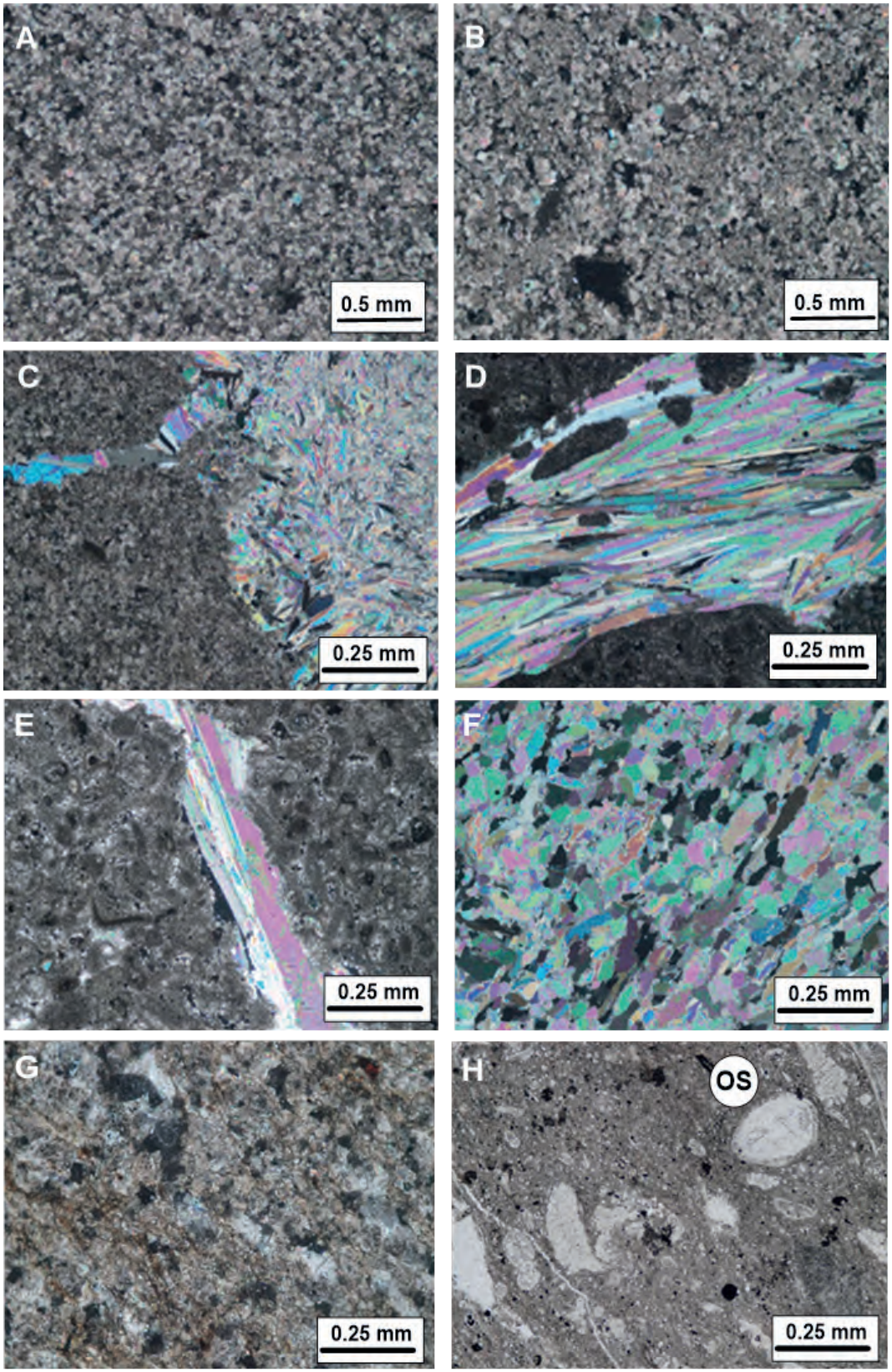


Fig. 4. The Paleocene (Selandian) Farrud Member microfacies; A-B, Foraminiferal bioclastic wackestone association. Foraminiferal (FO), algae (AL), echinoid (ECH), brachiopod (BR) and Nummulites (NU), sample 35 (5713 ft), GG1 well, PPL and XPL. C, Foraminiferal lime mud association, sample 34 (5670 ft), GG1 well, XPL. D-E, Ostracodal foraminiferal dolomitized packstone association. Gastropod (GA) and ostracod shells (OS), sample 33 (5668 ft), GG1 well, PPL and XPL. F-H, Echinoidal oolitic foraminiferal dolomicrite association. Oolite (OO), echinoid spines (ECH), algae (AL), gastropod (GA), bivalve (BI), brachiopod (BR) and bryozoan (BRY), samples 54-50 (5337-5322 ft), LLL1 well, PPL and XPL.

energetic conditions, with fluctuating sea level due to the prevalence of micrite. This microfacies is similar to SMF8 and FZ7 (Wilson, 1975; Flügel, 2004).

***Foraminiferal biomicrite association/ Foraminiferal wackestone (Figs. 4A & B, sample 35, GG1 well)***: Abundant allochems and ill-defined planktonic and benthic foraminiferal chambers are loosely packed. Pelecypod fragments and foliated brachiopods, algae, gastropods commonly float within lime mud micritic matrix. Most allochems boundaries are admixed within the rock matrix assuming a partial micritization. Diagenesis is recorded by recrystallization of mosaic coarse grained calcite within the internal structure of the fossils and inside the empty patches. Deposition took place within relatively quiet, less energetic conditions most likely below wave base conditions (quiet inner-shelf marine conditions). It resemnbles SMF9 and FZ7 (Wilson, 1975; Flügel, 2004).

***Foraminiferal biomicrite association/ Foraminiferal lime-mud (Fig. 4C, sample 34, GG1 well)***: Fine-grained crystalline micrite is the major constituent. Allochems are represented by ill-defined scattered foraminiferal tests. The boundaries of allochems are deformed and admixed within the rock matrix. Diagenesis took place due to micritization. Deposition prevailed in relatively quiet, less energetic conditions below wave base (quiet inner-shelf marine conditions). This facies is similar to SMF9 and FZ7 (Wilson, 1975; Flügel, 2004).

***Ostracodal foraminiferal dolostone association/ Ostracodal, foraminiferal packstone (Figs. 4D & E, sample 33, GG1 well)***: Coarse-grained rhombic dolomite is surrounded by remains of fine-grained crystalline micrite as a major constituent. Allochems represented by complete ostracodal shells, ill-defined foraminiferal chambers, gastropods and carbonate fragment. The internal cavity of the shell is entirely recrystallized into coarse crystalline mosaic calcite. Diagenesis is evidenced by micritization process, well developed mosaic calcite crystals seen inside fossil cavities, indicate active recrystallization. Dolomitization is recorded by the development of dolomite surrounding the allochems at the expense of lime due to the high Mg-rich marine pore-water invading the rock. Deposition took place within relatively intertidal flats under marked shallow marine, less energetic conditions with fluctuating sea level. This facies is similar to SMF12 and FZ6.

***Echinoidal oolitic foraminiferal dolomicrite association/Echinoidal, foraminiferal packstone (Figs. 4F-H and Figs. 5A-C, samples 54-50, LLL1 well)***: Coarse interlocking mosaic dolomite and micrite matrix. Abundant allochems represented by echinoid spines, concentric oolites, pelloids, bryozoans, algae, foraminifera, bivalves, gastropods, brachiopods and shell fragments, cemented by sparry mosaic calcite and/or crystallized dolomites. Diagenesis is caused by the dissolution of micritic matrix and large carbonate fragments replaced by coarse- grained sparry calcite and well developed dolomite. Deposition prevailed within warm, marine setting of fluctuating sea level. An intertidal foreshore lagoonal setting is suggested for this association, which correlates SMF 12 and FZ 6 (Wilson, 1975; Flügel, 2004).

***Gypsiferous dolostone association/Gypsum dolomite wackestone (Figs. 5D & E, samples 49-48, LLL1 well)***: Uni-sized medium-grained mosaic euhedral dolomite crystals. Allochems are rare represented by ill-defined scattered bivalves floating within the dolomitic groundmass. Pale yellow colored patches and irregular lamina of gypsum are seen. The abundance of uni-sized homogeneous rhomboid dolomite crystals suggests deposition within arid, evaporitic tidal flats to supratidal setting. The occurrence of gypsum indicates close nearness to super-saturated saline-rich source together with high temperature conditions. This facies resembles SMF23 and FZ9 (Wilson, 1975; Flügel , 2004).

***Foraminiferal dolomitized micrite association/ Foraminiferal dolomitic packstone (Fig. 5F, sample 47, LLL1 well)***: Fine to coarse dolomitic matrix with abundant compact allochems. The allochems are represented by foraminifera, brachiopods, pelloids and oolites cemented with developed euhedral fine to medium-grained recrystallized dolomite. Some of allochems are totally dissolved and replaced by recrystallized mosaic sparry calcite. The dolomitization is at the expense of micrite due to Mg-rich solution invading the pore spaces of the rock. Deposition took place within a relatively quiet and less energetic lagoonal setting. This facies resembles SMF9 and FZ6.

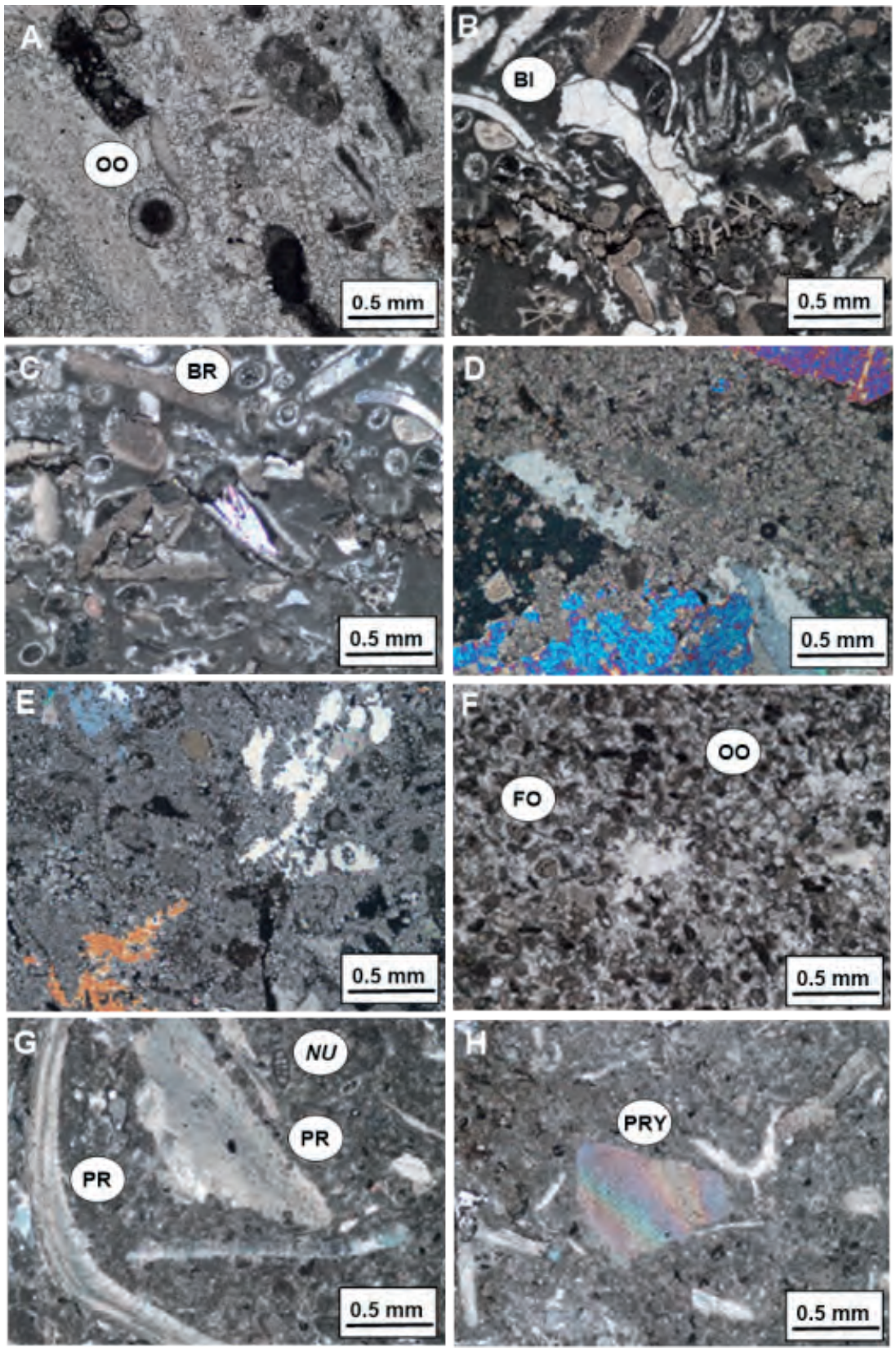


Fig. 5. The Paleocene (Selandian) Farrud Member microfacies; A-C, Echinoidal oolitic foraminiferal dolomicrite association. Oolite (OO), echinoid spines (ECH), algae (AL), gastropod (GA), bivalve (BI), brachiopod (BR) and bryozoan (BRY), samples 54-50 (5337-5322 ft), LLL1 well, PPL and XPL. D-E, Gypsum dolomite wackestone association, samples 49 (5317 ft) and 48 (5314 ft), LLL1 well, XPL. F, Foraminiferal dolomite packestone association. Foraminifera (FO) and oolite (OO), sample 47 (5304 ft), LLL1 well, PPL. G-H, Foraminiferal brachiopod biomicrite association. Nummulites (NU), bivalve (BI), brachiopod (BR) and bryozoan (BRY), sample 21, 6003 ft, RRR1 well, XPL.

***Foraminiferal brachiopod biomicrite association/ Foraminiferal bioclasts floatstone (Figs. 5G & H and Fig. 6A, sample 21; Fig. 6B-C, samples 20-18, RRR1 well)***: Fine-grained cryptocrystalline micritic matrix enriched with allochems of different varieties. The allochems are represented by different foraminiferal tests (miliolids and nummulites), various debris of bivalves and gastropods, oyster and pelecypod fragments. Other allochems include calcareous algae (Halimeda), bryozoa and ostracodal valves, which float in the micritic matrix. The oysters have foliated internal structure with thick shells. Diagenesis is seen due to micritization and dissolution of quartz boundaries replaced by micrite. Sometimes recrystallization of coarse sparry calcite is well developed. Deposition prevailed within relatively quiet, an inner shelf, shallow marine conditions and diminishing energy below wave base level. This facies resembles SMF9 and FZ7 (Wilson, 1975; Flügel, 2004).

***Gypsiferous micrite association/Gypsum lime-mudstone (Figs. 6D & E, sample 18, RRR1 well):*** Lime-mud (micrite) groundmass of very fine cryptocrystalline carbonate materials. Allochems not present. Faint pale yellow colored patches and irregular laminae of gypsum occupying a large area within the matrix. Deposition prevailed in less energetic marine conditions due to dominance of micrite. However, the development of gypsum at the expense of lime-mud indicates saturated saline solution. This occurs under fluctuating sea level conditions into intertidal foreshore lagoonal setting. This association matches SMF23 and FZ8 (Wilson, 1975; Flügel, 2004).

***Echinoid oobiosparite association/Oolitic biosparite packstone (Figs. 6F & G, samples 17-16, RRR1 well)***: Different varieties of allochems are cemented with drusy mosaic equant calcite crystals. Allochems include abundant concentric oolites, echinoids, algae, micrite peloids and foraminifera (e.g. nummulites and miliolids). Most allochems show micritic envelope and the internal cavity of the shells is entirely recrystallized into mosaic calcite.Deposition took place within relatively shallow agitated marine conditions in the outer shelf bays. However, oolites originated within shoals near outer platform margins.This facies is equivalent to SMF15 and FZ8 (Wilson, 1975; Flügel, 2004).

***Foraminiferal quartz biomicrite association/ Foraminifertal quartz wackestone (Fig. 6H and Fig. 7A, sample 15, RRR1 well)***: Dark brown cryptocrystalline argillaceous micritic matrix with few allochems representedby ill-defined foraminifera. Nummulites and miliolids can be seen, although most fossils are altered and replaced by crystalline mosaic quartz. Some patches of the micritic matrix are dissolved and replaced by drusy megaquartz, indicative of slicicfication as a late stage diagenesis. Deposition prevailed within shallow marine conditions under mid to outer shelf setting. This association matches SMF9 and FZ7 (Wilson, 1975; Flügel, 2004).

***Evaporite association (Fig. 7B, sample 14, RRR1 well)***: Medium to fine-grained gypsum and anhydrite laths are arranged in foliated layers and random aggregate structures. Recrystallization of anhydrites shows equant and lath crystals producing coarse granular mosaic and large fibrous crystals. This indicates a direct precipitation of sulphate from water in a relatively tidal flat of diminishing energy conditions. The evaporite facies suggests close nearness to super-saturated saline-rich sources of high intertidal-supratidal flats, together with high temperature conditions (Kinsman, 1969).

***Pelagic foraminiferal biomicrite association/ Foraminiferal packstone (Fig. 7C, sample 13, RRR40 well)***: Fine cryptocrystalline micrite mixed with clay material as matrix. Allochems are grain-supported, represented by ill-defined scattered foraminiferal chambers with deformed boundaries and admixed within the micritic matrix. Allochems consist of dominant microscopic foraminiferal tests, echinoids, ostracods, algae, bryozoa and bivalve fragments. Iron patches and pellets are scattered in the matrix. Most fissures are filled with sparry calcite cement. This kind of microfacies suggests deposition in quiet less energetic marine conditions due to dominance of micrite. Mid to outer shelf marine setting is suggested for this facies. This association matches SMF3 and FZ1 (Wilson, 1975; Flügel, 2004).

***Brachipods bivalves biomicrite association/ Brachipod bivalves packstone (Figs. 7D & E, sample 12, RRR40 well)***: Cryptocrystalline micritic matrix enriched with different varieties of allochems. The allochems include foraminiferal

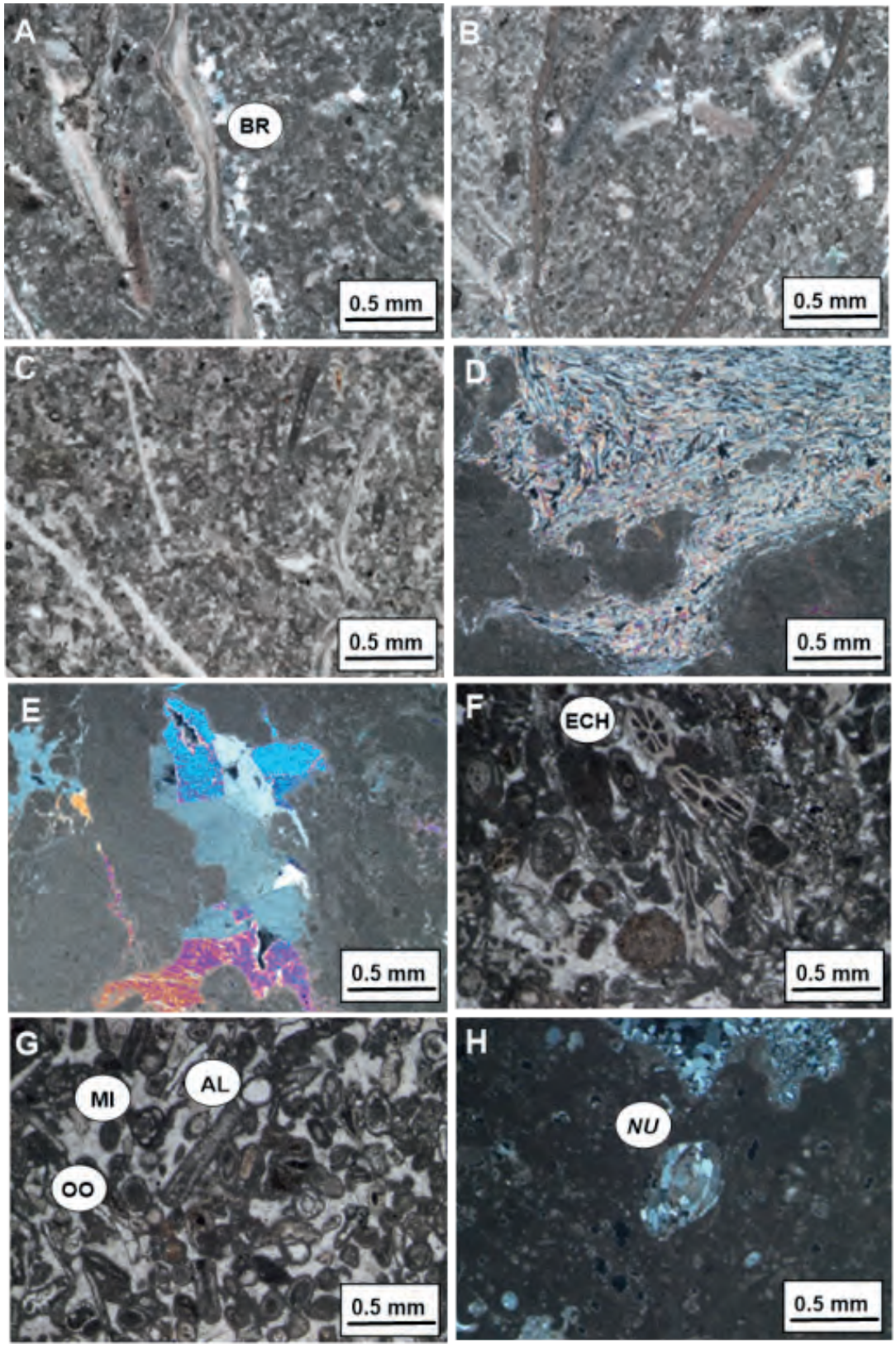


Fig. 6. The Paleocene (Selandian) Farrud Member microfacies; A, Foraminiferal brachiopod biomicrite association. brachiopod (BR), sample 21 (6003 ft), RRR1 well, XPL. B-C, Photomicrographs in PPL showing foraminiferal brachiopod biomicrite association/ foraminiferal bioclasts floatstone, sample 20 (5994 ft) and sample 19 (5993 ft), RRR1 well, PPL. D-E, Gypsiferous micrite association, sample 18 (5984 ft), RRR1 well, XPL. F-G, Echinoid oobiosparte association/oolitic biosparite packstone. Oolite (OO), echinoid (ECH), algae (AL) and miliolid (MI), sample 17 (5981 ft); sample 16 (5970 ft), RRR1 well, XPL. H, Foraminiferal quartz biomicrite association. Nummulites (NU), sample 15 (5954 ft), RRR1 well, XPL.

tests assigned to miliolids, nummulites, and pelagic foraminifera. Other structures include brachiopod fragments, long straight bivalve and gastropod shell fragments, oysters with foliated internal structure, pelecypod fragments, algae (halimeda), brayozoa and ostracodal valves. Deposition took place within relatively quiet, less energetic shallow marine conditions below wave base level and an inner shelf marine setting is suggested. This facies resembles SMF9 and FZ7 (Wilson, 1975; Flügel, 2004) respectively.

***Oolitic bivalve algal foraminiferal biomicrite association/Oolitic bivalve foraminiferal packstone (Figs. 7F-H and Fig. 8A, samples 10-11, RRR40 well)***: Highly fossiliferous, tightly packed bioclasts of sand and pebbly-sized skeletal and non-skeletal debris are admixed in compacted micritic matrix. The allochems encounter concentric and radial oolites, bivalves, algae, foraminifera (nummulites and miliolids), echinoids, bryozoa, brachiopopds and oysters. Dissolution of some patches of the micrite was replaced by coarse-grained mosaic calcite as a common diagenesis. Deposition prevailed in relatively less agitated marine conditions within mid-outer shelf marine setting below wave base as this facies corresponds to SMF12 and FZ6 (Wilson, 1975; Flügel, 2004).

***Argillaceous biomicrite association/Brachipod bivalves lime-mudstone (Figs. 8B & C, sample 9, RRR40 well)***: Cryptocrystalline argillaceous micritic matrix compacted and laminated. The allochems include bivalves, brachiopods, foraminifera, gastropod fragments and algae. Deposition took place in relatively quiet less energetic marine conditions under fluctuating sea level, as evidenced by dominance of micrite/ shale intercalation. Shallow inner shelf bayment is suggested for this facies. This facies resembles SMF9 and FZ7.

***Pelagic foramineral argillaceous biomicrite association/Pelagic foraminiferal lime-mudstone (Figs. 8D-F, sample 32, RRR45 well; Fig. 9E, sample 26, RRR45 well)***: Fine-grained cryptocrystalline argillaceous micritic matrix slightly laminated with scattered poorly-preserved foraminiferal tests, strongly micritzed and admixed with the matrix. Deposition took place in quiet less energetic marine conditions due to dominance of micrite. Mid to outer shelf marine setting is suggested for this facies. This association is concomittant with SMF3 and FZ1 (Wilson, 1975; Flügel, 2004).

***Fossiliferous biomicrite association/Foraminiferal bivalves packstone (Figs. 8F-H and Fig. 9A, samples 31-29, RRR45 well; Fig. 9B & C, sample 28, RRR45 well)***: Argillaceous micritic matrix is enriched in allochems of sand and pebbly sized skeletal and non-skeletal debris. Allochems include foraminifera (nummulites and miliolids), algae, bryozoa, pelecypods, oolites, echinoids, oysters, brachiopods, concentric oolites and gastropods embedded in a carbonate mud matrix. Diagenesis is due to crystallization of coarse-grained sparry mosaic calcite in some patches at the expense of micrite matrix. Deposition might have taken place within less energetic nearness to mid-outer shelf marine setting. This association is close to SMF12 and FZ6 (Wilson, 1975; Flügel, 2004).

***Dolomitized dismicrite association/Dolomitized wackestone (Fig. 9D-F, samples 25 & 27, RRR45 well)***: Petrogtaphically, the rock is entirely composed of fine-grained, non-ferroan subhedral to anhedral dolomite crystals surrounded by micrite. The most common diagenetic event is the development of dolomite at the expense of micrite. Dolomitization took place under Mg-rich marine water that invaded the original dismicrite. Deposition indicates an intertidal foreshore lagoonal setting. This association is concordant with SMF25 and FZ8 (Wilson, 1975; Flügel, 2004).

***Gypsiferous dismicrite association/Gypsiferous lime-mudstone (Fig. 9G, sample 24, RRR45 well)***: This association is entirely composed of framework of fine to very fine-grained micritic matrix. No allochems are seen, however, some fossils show badly preserved. Large area was attacked by sulphate solution that crystallized as irregular, faint pale yellow crystal laths of gypsum which occupy large area within the association. Deposition prevailed in intertidal to lagoonal conditions. This association resembles SMF23 and FZ8 (Wilson, 1975; Flügel, 2004).

***Gastropods dolomitized micrite association/ Gastropods dolomitic lime-mudstone (Fig. 9H, sample 23, RRR45 well)***: Cryptocrystalline micritic matrix with few allochems is formed of ill-defined gastropods, foraminiferal tests and carbonate

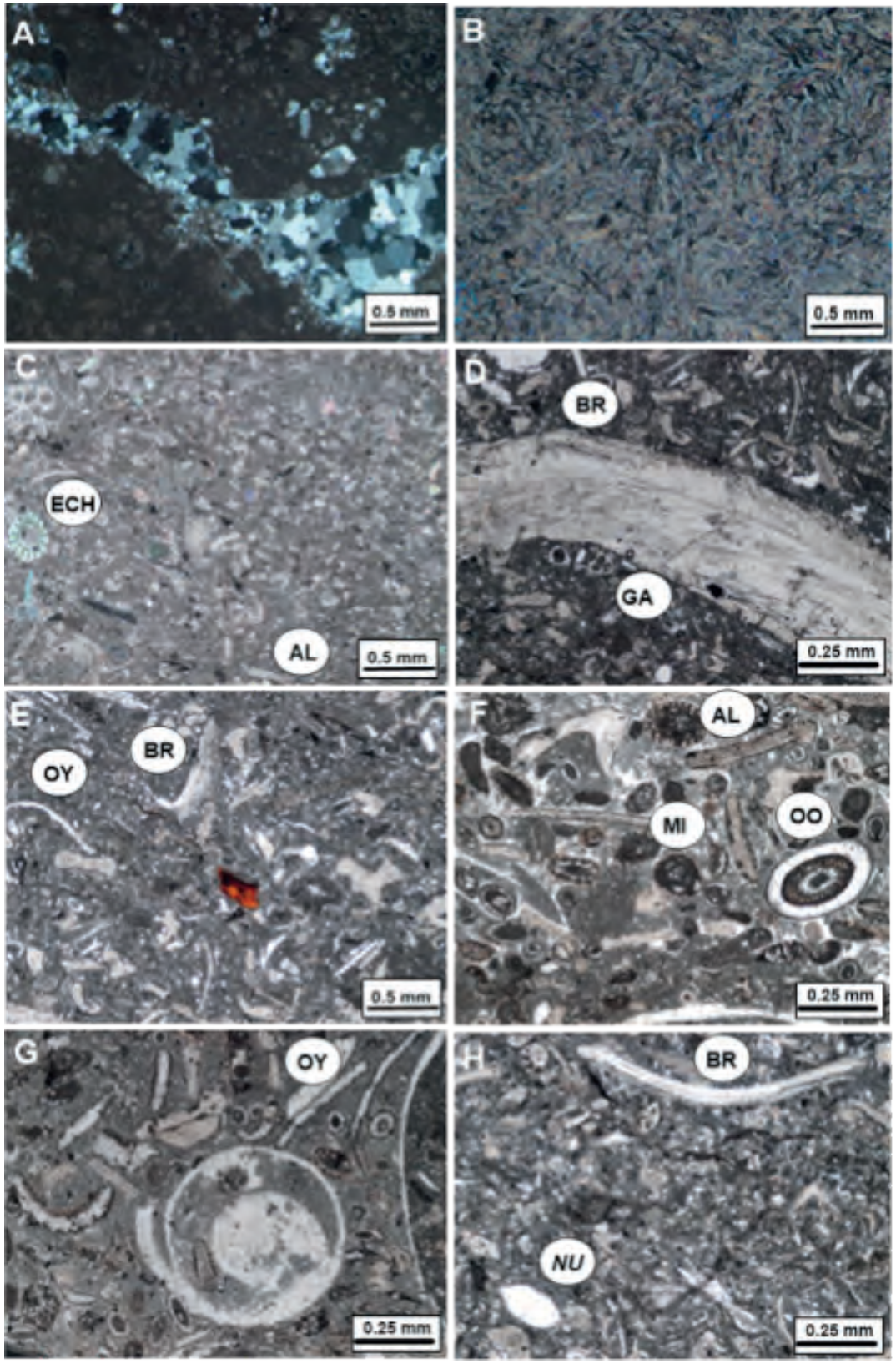


Fig. 7. The Paleocene (Selandian) Farrud Member microfacies; A, Foraminiferal quartz biomicrite association, sample 15 (5954 ft), RRR1 well, XPL. B, Evaporite association, sample 14 (5951 ft), RRR1 well, XPL. C, Pelagic foraminiferal biomicrite association. Echinoid (ECH) and algae (AL), sample 13 (6048 ft), RRR40 well, PPL. D-E, Brachiopods bivalves biomicrite association. Brachiopod (BR), oyster (OY) and gastropod (GA), sample 12 (6041 ft), RRR40 well, PPL. F-H, and Fig. 8. A, Oolitic bivalve algal foraminiferal biomicrite association. Oolite (OO), algae (AL), miliolid (MI), nummulites (NU), brachiopopd (BR) and oyster (OY), samples 11 (6035 ft); sample 10 (6032 ft), RRR40 well, PPL and XPL.

fragments cemented with dolomites. The internal cavity of the shells shows a partial micritization replaced by fine crystallized subhedral dolomite crystals. Deposition took place within warm, saline saturated marine setting. An intertidal foreshore lagoonal setting connected to the open sea is suggested. This association is similar to SMF23 and FZ9 (Wilson, 1975; Flügel, 2004).

***Evaporite assiciation (Fig. 10A, sample 22, RRR45 well)***: Fine crystalline fibrous crystals of faint pale yellow colored anhydrite and gypsum are arranged in foliated aggregates and/or irregular laminas. Deposition took place within intertidal-flat to supratidal setting close to super saturated saline-rich sources associated with high temperature conditions.

**Microfacies Characteristics of Lower Paleocene Mabruk (Selandian) Member**

Eight thin sections have been examined from the Middle Paleocene Mabruk Member in two wells, namely LLL1 (4 samples) and RRR40 (4 samples). These thin sections can be discussed herein as follow:

***Foraminiferal pelloidal biomicrite association/ Foraminiferal pellets wackestone (Fig. 10B, sample 4, RRR40 well)***: The thin section is composed of microcrystalline micrite as a framework matrix. Allochems are different and dominated by foraminifera chambers floating within the matrix. The allochems strongly admixed into the rock matrix assuming partial micritzation process accompanying the burial. The assimilated allochem boundaries strongly admixed into the rock matrix assume partial micritization process. Rare iron pockets and a few pellets are seen scattered in the association.

***Dismicrite association/Lime-mud (Fig. 10C & D, samples 2-3, RRR40 well)***: The groundmass is made up of lime-mud homogeneous micrite. No allochems are observed. The rock has been subjected to partial sparitization. Deposition prevailed in relatively quiet less agitated marine conditions (tidal flats to inner-shelf lagoon setting) due to dominance of micrite.

***Gypsiferous quartz arenite association (Fig. 10E & F, sample 1, RRR40 well)***: A groundmass is almost entirely composed of crystallized medium to fine-grained anhedral quartz crystals, partially and sometimes completely replaced by secondary sulphate minerals (anhydrite and gypsum). Deposition prevailed within tidal flats invaded by freshwater circulation.

***Gypsiferous dolomitized biomicrite association/ Gypsum dolomite wackestone (Figs. 10G-J, samples 6-8, LLL1 well)***: Medium to coarse-grained crystalline mosaic dolomite crystals replaced most of the biomicrite marix. Ill-defined allochems include foraminiferal tests, echinoids and algae. The groundmass is attacked by a sulphate solution, where fine crystalline fibrous gypsum and anhydrite laths partially replaced dolomite and filling the intergranular molidic porosity. Dolomitization and sulphanization are the most significant diagenetic processes that affected the rock. The abundance of rhomboid dolomite crystals suggests deposition within arid, evaporitic tidal flats, or supratidal setting. This facies matches SMF23 and FZ9 (Wilson, 1975; Flügel, 2004).

***Dolostone association/Dolomite floatstone (Fig. 10K, sample 5, LLL1well)***: A groundmass consists of coarse-grained, crystalline, well developed euhedral stained dolomite crystals. Irregular patches of faint grey gypsum are also observed. The abundance of uni-sized homogeneous rhomboid dolomite crystals suggests primary deposition from shallow restricted supratidal marine setting under high temperature. This association resembles SMF25 and FZ9 (Wilson, 1975; Flügel, 2004).

## CONCLUSIONS

Fifty four thin sections were investigated from the two members Farrud (Lower Paleocene) and Mabruk (Upper Paleocene) in six wells; QQQ1, GG1, LLL1, RRR1, RRR40 and RRR45. Sediments of this member consist mainly of limestone and/ or mixed dolomite, evaporite, limestone and argillaceous beds. The microfacies trends detected from the investigation of 46 core samples from Farrud Member indicate that the deposition was started within the realm of shallow supratidal and intertidal subenvironments where dolostone and evaporite facies deposited in the Farrud Member of wells QQQ1, LLL1 and RRR45. While deposition in wells; GG1, RRR1 and RRR40 exhibits different depositional trend where foraminiferal, brachiopods and bivalves biomicrite of different textures vary from lim-mudstone to wackestone and packstone associations. They indicate deposition

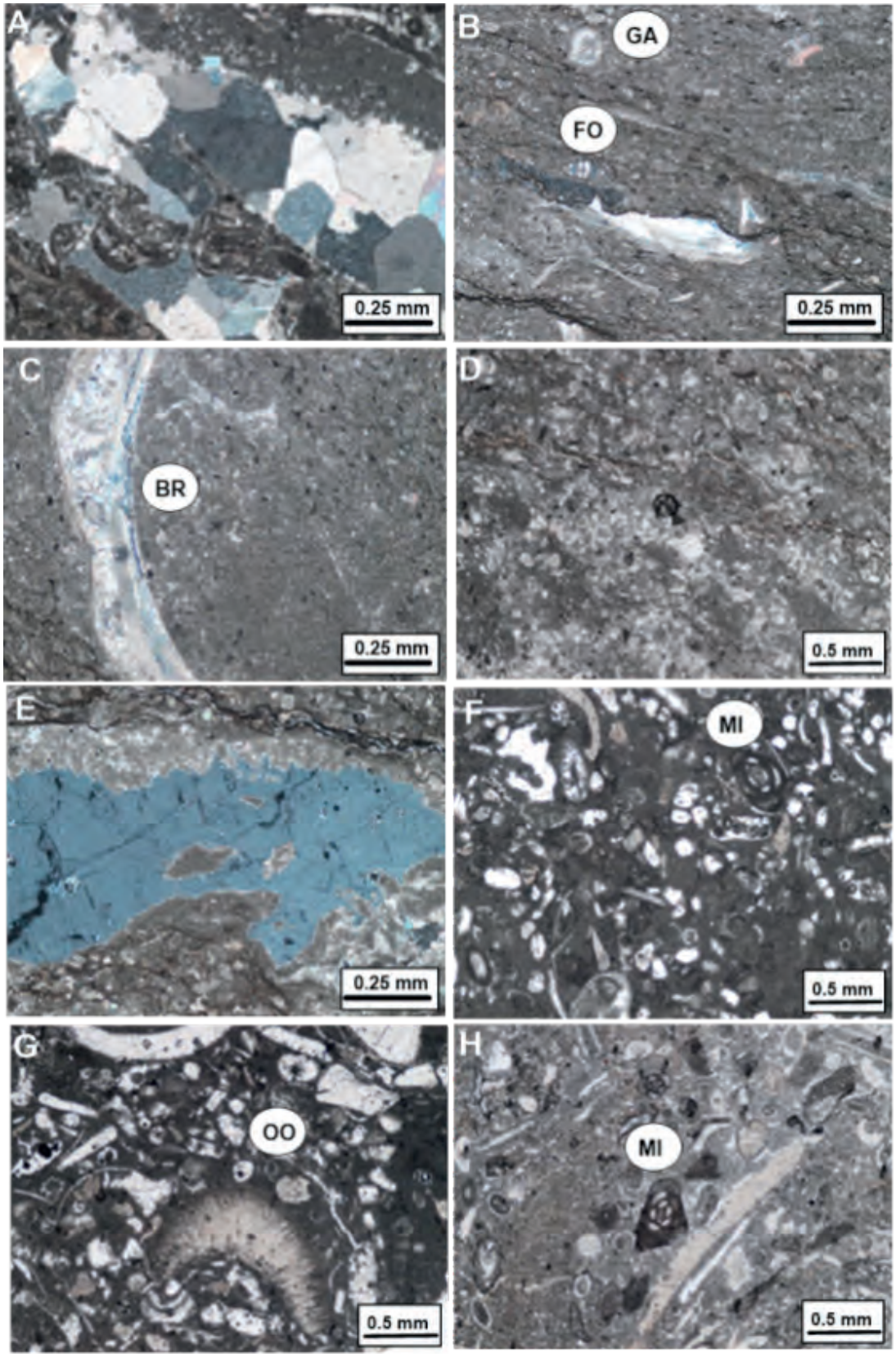


Fig. 8. The Paleocene (Selandian) Farrud Member microfacies; B-C, Brachiopods bivalves lime-mudstone association. Foraminifera (FO), gastropod fragment (GA) and brachiopod (BR), sample 9 (6029 ft), RRR40 well, XPL. D-E, Pelagic foraminiferal argillaceous biomicrite association, sample 32 (5959 ft), RRR45 well, PPL. F-H and Fig. 9. A, Foraminiferal bivalves bioclasts packstone association. Miliolid (MI), oolite (OO), algae (AL), oyster (OY) and gastropod (GA), samples 31 (5949 ft); 29 (5898 ft), RRR45 well, PPL and XPL.

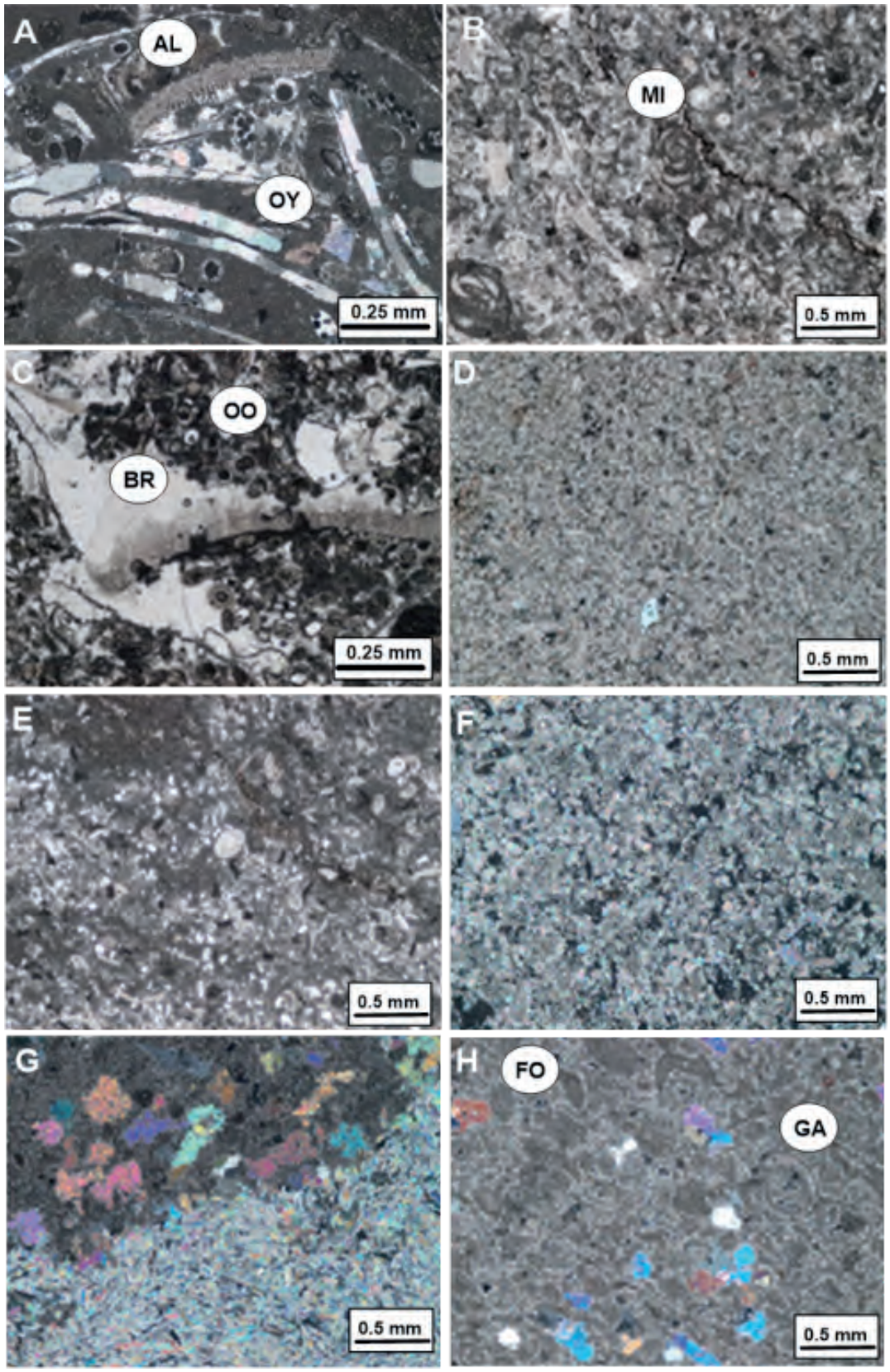


Fig. 9. The Paleocene (Selandian) Farrud Member microfacies; B-C, Foraminiferal bivalves bioclasts packstone association. Brachiopod (BR), oolite (OO) and miliolid (MI), sample 28 (5874 ft), RRR45 well, PPL. D-F, Dolomitization invaded the dismicrite, sample 27 (5861 ft); sample 25 (5850 ft), RRR45 well, PPL. E, Pelagic foraminiferal argillaceous biomicrite association, sample 26 (5857 ft), RRR45 well, PPL. G, Gypsiferous dismicrite association, sample 24 (5840 ft), RRR45 well, XPL. H, Gastropods dolomitized micrite association. Gasstropods (GA) and forminiferal tests (FO), sample 23 (5837 ft), RRR45 well, XPL.

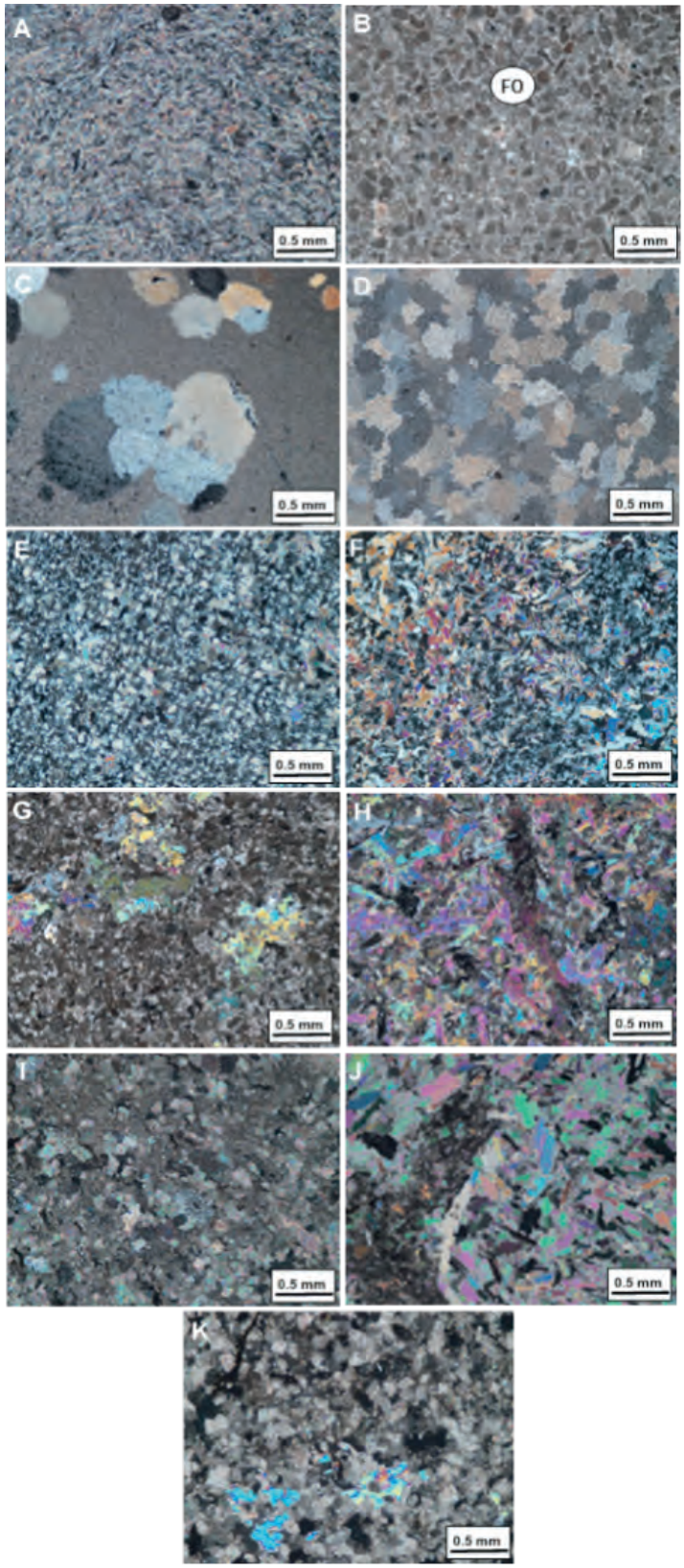


Fig. 10. The Paleocene (Selandian) Farrud Member microfacies; A, Evaporite association, sample 22 (5832 ft), RRR 45 well, XPL. The Paleocene (Selandian) Mabruk Member microfacies; B, Foraminiferal pelloidal biomicrite association. Foraminifera chambers (FO), sample 4 (5989 ft), RRR40 well, PPL. C-D, Dismicrite association, sample 3 (5978 ft); sample 2 (5972 ft), RRR40 well, XPL. E, Gypsiferous quartz arenite association, sample 1 (5968 ft), RRR40 well, XPL. F, Gypsiferous quartz arenite association, sample 1 (5968 ft), RRR40 well, XPL. G-J, Gypsiferous dolomitized biomicrite association, sample 8 (5298 ft); sample 7 (5297 ft); sample 6 (5289 ft), LLL1 well, XPL. K, Dolostone association, sample 5 (5280 ft), LLL1 well, XPL.

in mainly deeper environments of the shelf bays with maximum sea level rise during inner-shelf environment where fossiliferous bioclastic packestone was dominated. On the other hand, some wells exhibit different deposition in Farrud Member probably due to their locations in the basin of deposition. They reflect rapid oscillation of the sea level marked by drop land-ward shift of the sea shore deposition prevailed by supratidal gypsiferous dolostone and numerous ferrugineous materials as clouds staining many parts of dolomite and surrounded the micritized fossils. This situation ends the deposition of the Farrud Member in most of the studied wells. On the other hand, the facies in the northern part of the Concession -11 field indicates deposition in deeper marine setting than in the southern facies.

Mabruk Member (Upper Paleocene) overlies Farrud Member in two wells of the concession 11. It is generally limestone/dolomite dominated facies intercalated with evoporites and thin siliciclastics. Generally, these facies indicate deposition started during a phase of sea level drop resulted in the dominance of shallow intertidal, supratidal facies instead of the marked deeper shelf marine conditions. 8 core samples representing Mabruk Member were investigated from two wells LLL1 and RRR40. Mabruk Member reflects paleoenvironmental trends marked by sea level fluctuations accompanied with a relatively marine shelf bay conditions intervened with short-lived shallow intertidal and supratidal warm coastal sedimentation. As a result dolostone, evaporitic dismicrites and gypsiferous dolostone of supratidal characters were deposited.

## ACKNOWLEDGEMENTS

We are indebted to Harouge Oil Operations for the provision of samples, geological information and permission to publish this study.

## REFERENCES

Abadi, A. M. (2002). Tectonics of the Sirt Basin. Unpublished PhD Dissertation, Vrije Universiteit, Amsterdam ITC. Enschede, 187p.

Abadi, A. M.; Van Wees, J-D.; van Dijk, P.M. and Cloetingh, S. A. P. L. (2008). Tectonics and Subsidence Evolution of the Sirt Basin, Libya. AAPG Bulletin, 92(8): 993-1027.

Abugares, M. M. (2007). Deposition, Development of the Cretaceous Lidam Formation, SE Sirt Basin, Libya. Unpublished M. Sc. Thesis, Durham University, 217p.

Adams, A. E.; Mackenzie, W. S. and Guilford, C. (1984). Atlas of Sedimentary Rock Under the Microscope. Harlow-Longman Scientific and Technical, John Wiley and Sons, Inc., New York, 104p.

Ahlbrandt, T. S. (2001). The Sirt Basin Province of Libya-Sirte-Zelten Total Petroleum System. U.S. Geological Survey, Bulletin 2202-F: 29p.

Barr, F. T. and Weegar, A. A. (1972). Stratigraphic Nomenclature of the Sirte Basin, Libya. Petroleum Exploration Society of Libya, Tripoli: 179p.

Carr, I. D. (2003). A Sequence Stratigraphic Synthesis of the North African Mesozoic. Jour. Petr. Geol., 26: 133-152.

Dunham, R. J. (1962). Classification of Carbonate Rocks According to Their Depositional Texture. In: Classification of carbonate rocks (Ed. by: W. E. Ham). AAPG Memoir 1: 108-121.

Embry, A. F. and Klovan, J. E. (1971). A Late Devonian Reef Tract on Northeastern Banks Island. N. W. T. Cana. Petr. Geol., Bulletin, 19(4): 730-781.

Flügel, E. (1982). Microfacies Analysis of Limestones. Springer -Verlag, Berlin, 633p.

Flügel, E. (2004). Microfacies of Carbonate Rocks: Analysis, Interpretation and Application. Springer-Verlag, Berlin-Heidelberg-New York, 976p.

Folk, R. L. (1959). Practical Petrographic Classification of Limestone. AAPG, Bulletin, 43: 1-38.

Folk, R. L. (1962). Spectral Subdivision of Limestone Types. In: Classification of carbonate rocks (Ed. by: W. E. Ham). AAPG Memoir 1: 62-85.

Gras, R. and Thusu, B. (1998). Trap Architecture of the Early Cretaceous Sarir Sandstone in the Eastern Sirt Basin, Libya. In: Petroleum Geology of North Africa (Ed. by: D. S. MacGregor; R. T. J. Moody and D. D. Clark-Lowes). Geol. Soc., Spec. Publ. 132: 317-334.

Gumati, Y. D. and Kanes, W. H. (1985). Early Tettiary Subsidence and Sedimentary Facies, Northern Sirt Basin, Libya. AAPG, Bulletin 69(1): 39-52.

Hallett, D. (2002). Petroleum Geology of Libya. Elsevier, Amsterdam, 503p.

Harouge Oil Operations (HOO), Libya (2009). Unpublished Internal report: 80p.

Kinsman, D. J. (1969). Interpretation of Sr+2 Concentration in Carbonate Minerals and Rocks. Jour. Sedi. Petro., 39(2): 486-508.

Reading, H. G. (1996). Sedimentary Environments: Processes, Facies and Stratigraphy, 3rd edn. Blackwell Science, Oxford, 688p.

Selley, R. C. (1980). Ancient Sedimentary Environments. Chapman and Hall, 287p.

Wilson, J. L. (1975). Carbonate Facies in Geologic History. Spring-Verlag, New York, Heidelberg, Berlin, 471p.